Received: 8 February 2022 | Revised: 26 May 2022 | Accepted: 19 June 2022

DOI: 10.1002/pca.3163

RESEARCH ARTICLE

Phytochemical Analysis WILEY

New insights into the Van Krevelen diagram: Automated molecular formula determination from HRMS for a large chemical profiling of lichen extracts

Simon Ollivier[1,2] | Philippe Jéhan[1] | Damien Olivier-Jimenez[2] | Fabian Lambert[1] | Joël Boustie[2] | Françoise Lohézic-Le Dévéhat[2] | Nicolas Le Yondre[1]

[1]CNRS, ScanMAT UAR 2025, CRMPO (Centre Régional de Mesures Physiques de l'Ouest), Univ Rennes, Rennes, France

[2]CNRS, ISCR (Institut des Sciences Chimiques de Rennes) - UMR 6226, Univ Rennes, Rennes, France

Correspondence
Dr. Nicolas Le Yondre, Univ Rennes, CNRS, ScanMAT UAR 2025, CRMPO (Centre Régional de Mesures Physiques de l'Ouest), F-35000 Rennes, France.
Email: nicolas.leyondre@univ-rennes1.fr

Dr. Françoise Lohézic-Le Dévéhat, Univ Rennes, CNRS, ISCR (Institut des Sciences Chimiques de Rennes) - UMR 6226, F-35000 Rennes, France.
Email: francoise.le-devehat@univ-rennes1.fr

Present address
Simon Ollivier, INRAE, UR BIA, F-44300 Nantes, France and INRAE, PROBE research infrastructure, BIBS facility, F-44300, Nantes, France

Abstract

Introduction: In recent years, LC-MS has become the golden standard for metabolomic studies. Indeed, LC is relatively easy to couple with the soft electrospray ionization. As a consequence, many tools have been developed for the structural annotation of tandem mass spectra. However, it is sometimes difficult to do data-dependent acquisition (DDA), especially when developing new methods that stray from the classical LC-MS workflow.

Objective: An old tool from petroleomics that has recently gained popularity in metabolomics, the Van Krevelen diagram, is adapted for an overview of the molecular diversity profile in lichens through high-resolution mass spectrometry (HRMS).

Methods: A new method is benchmarked against the state-of-the-art classification tool ClassyFire using a database containing most known lichen metabolites (n ≈ 2,000). Four lichens known for their contrasted chemical composition were selected, and extractions with apolar, aprotic polar, and protic polar solvents were performed to cover a wide range of polarities. Extracts were analyzed with direct infusion electrospray ionization mass spectrometry (DI-ESI-MS) and atmospheric solids analysis probe mass spectrometry (ASAP-MS) techniques to be compared with the chemical composition described in the literature.

Results: The most common lichen metabolites were efficiently classified, with more than 90% of the molecules in some classes being matched with ClassyFire. Results from this method are consistent with the various extraction protocols in the present case study.

Conclusion: This approach is a rapid and efficient tool to gain structural insight regarding lichen metabolites analyzed by HRMS without relying on DDA by

LC-MS/MS analysis. It may notably be of use during the development phase of novel MS-based metabolomic approaches.

KEYWORDS
extract comparison, lichens, metabolomics, structural classification

1 | INTRODUCTION

In recent years, significant advances in mass spectrometry (MS) have led to an increase in the measurement precision, sensitivity, and frequency of acquisition of tandem mass spectra. These different parameters, combined with the extensive separation capabilities of liquid chromatography, have made LC-MS the golden standard in metabolomics.[1,2] It is indeed a preferred analytical technique because it provides an insight into the composition of an extract in a form that could then be used by the industry.[3] However, this also implies (1) that a time-consuming extraction step must first be carried out and (2) that a certain number of compounds will not be detected because they will be retained on the column during separation. The extraction step determines, through the choice of solvent, the fraction of the metabolome that can be studied.[4] To obtain a more comprehensive insight into the chemical composition of an organism, it becomes necessary to perform various extraction steps, which further increases the workload. Therefore, it is interesting to develop new tools for a comprehensive understanding of this composition by directly analyzing the biological material. Natural products (NPs), which are the first historical source of drugs and remain an important subject of study for the pharmaceutical industry today,[5] are of special concern.

With the establishment of LC-MS as a standard for metabolomics, many biocomputing tools have been developed and combined to facilitate the processing and interpretation of the massive amounts of data generated.[6] Most, if not all, of these tools have been created to process data containing tandem mass spectra, which are commonly acquired in data-dependent acquisition (DDA).[7] It is possible to isolate features characterized by a dataset each comprising one *m/z* value, one retention time, and one tandem mass spectrum, which can be linked together by scores or shared patterns, notably on the GNPS platform.[8–10] Finally, these tandem mass spectra allow to propose identifications of a substantial number of molecules for each sample by comparing them with experimental[11,12] or *in silico* databases.[13] This structural annotation can allow a hierarchical classification of the molecules composing an extract, in particular thanks to the ClassyFire tool.[14]

The use of tandem mass spectra, while being the strength of these tools, is also their weakness. For instance, when developing new MS tools, it is not always possible to proceed *ab initio* to such an acquisition associating mass and tandem mass spectra. Data-independent acquisition is also possible and fragments all ions present in a wide range of *m/z* values regardless of intensity. However, it then becomes difficult to interpret the resulting multiplexed spectra, and the *ad hoc* algorithms require substantial computation time, which is not suitable for a rapid screening.[15] As an alternative, the option was to develop a tool providing structural insight directly from the molecular formula (MF), which can readily be computed from high-resolution MS data.[16] Indeed, an old tool from petroleomics – the Van Krevelen (VK) diagram[17] – was previously used to estimate the structural class associated with an MF through element ratios, notably for studying the composition of some alcohols.[18,19] To avoid the computational burden of MF determination, a local database search can be performed to determine element ratios for VK analysis;[20] however, in this approach the analysis ignores masses absent from the database, which can be problematic in a compound discovery context. Furthermore, a database search can sometimes generate mismatches because of cation adducts or the presence of "atypical" atoms – e.g., chlorinated metabolites, often described in lichens[21] – so, direct MF computation was chosen. For users wishing to try this kind of VK-based approach, a Python package (PyKrev) has recently been published and offers a number of processing options, including a classification function – but not tailored for phytochemicals.[22]

Lichens, as organisms constituted of a fungus living in a symbiotic relationship with an alga and/or a cyanobacterium,[23] possess an original chemistry comprising varied and unique compounds[21] and are thus well suited for the development and assessment of such a tool. They are also an interesting source of bioactive compounds,[24,25] and have been shown to be the ancestors of major fungal lineages (e.g., *Penicillium* spp., *Aspergillus* spp.).[26]

This paper is the first part of a study aiming to establish a novel concept using ambient MS for NP research, focused on four lichen species: *Evernia prunastri* (L.) Ach., *Lichina pygmaea* (Lightf.) C. Agardh., *Parmelia saxatilis* (L.) Ach., and *Roccella fuciformis* (L.) DC. The lichens were selected for their chemical diversity. An extensive list of the metabolites described in these species is provided as Table S1. In this paper a method capable of obtaining large structural insights into the composition of lichen extracts is presented without being reliant on tandem mass spectra.

2 | EXPERIMENTAL PROCEDURES

2.1 | General procedures

All solvents and reagents used in this study were HPLC grade (Sigma-Aldrich) and were used without further purification. In order to avoid any contamination by plastic compounds, the use of glass containers was preferred and the use of colored plastics was strictly prohibited. Eppendorf micropipetting systems were used for metering the extract

solutions. For experiments requiring the thermal desorption of extracts, samples were deposited on Marienfeld melting point capillaries.

2.2 | Lichen material

This study was conducted on herbarium specimens. They were collected in: Cressensac, France (N 45°0′19.321″ O 1°30′51.191″), August 2006 for *E. prunastri*; Roscoff, France (N 48°43′31.458″ O 3°58′8.651″), June 2016 for *L. pygmaea*; Girona, Spain (N 42°27′53.399″ O 1°47′23.816″), July 2017 for *P. saxatilis*; and Saint-Coulomb, France (N 48°41′29.299″ O 1°56′45.855″), May 2003 for *R. fuciformis*. Voucher specimens are kept in the herbarium of the University of Rennes, France under the respective reference codes: JB/06/51, JB/16/204, JB/17/213, and JB/03/02.

2.3 | Extraction protocol

The dried weights were optimized for each extraction to reach a sufficient quantity of material for all analyses (Figure S1). For each lichen, two extracts were obtained with methanol and acetone, and two extracts were from a successive extraction using cyclohexane, acetone, and then methanol (CAM) and using cyclohexane, acetone, and then water (CAW). CAM and CAW extracts were recombined pro rata to the extracted quantities. The selected quantities were 2 g for both the single-step "acetone" and the multiple-step "CAM" extracts, 500 mg for the "methanol" extract, and 4 g for the "CAW" extract. All extractions were performed using an Accelerated Speed Extractor Büchi SpeedExtractor E-914 after dispersion of ground lichens in celite (1:1 ratio, w/w). A 2-g sand bed made of Büchi quartz sand of 0.3–0.9 mm granulometry was used to avoid clogging of the sintered part of the extraction cartridges. Each extraction step consisted of three maceration cycles of 10 min in 40°C solvent, with a discharge time of 2 min and a degassing step between every cycle.

2.4 | HRMS analyses

Direct infusion electrospray MS (DI-ESI-MS) analyses were conducted on a Q-Exactive mass spectrometer (Thermo Scientific, Bremen, Germany) equipped with a Thermo HESI-II ion source. DI-ESI-MS analyses were performed on 15 µg/mL extract solutions using two ionization solvents, acetone and methanol. Acquisition time was set to 2 min (230 scans). Optimized parameters included a sheath gas set at 20 a.u., a transfer capillary voltage of 2,800 V, and an S-lens RF level of 50 a.u. The other parameters were set to default. The Thermo Scientific Q-Exactive™ was calibrated with Pierce LTQ Velos ESI Positive and Negative Ion calibration solutions and lock-mass calibration was applied on palmitic acid during acquisition (deprotonated molecule $[M\text{-}H]^-$ *m/z* 255.2330 and protonated molecule $[M + H]^+$ *m/z* 257.2475). Experiments were performed in a single batch with analytical triplicates. The system was rinsed with the working solvent up to noise level between each sample. No loss of sensitivity was observed when rerunning samples as control.

Atmospheric solids analysis probe MS (ASAP-MS) analyses were acquired on a Maxis 4G spectrometer (Bruker Daltonics, Bremen, Germany) equipped with an APCI ion source and a direct insertion probe. The extracts were deposited on Marienfeld melting point capillaries as homogeneous solutions and dried with nitrogen before insertion in the APCI source. Preliminary tests having shown a major thermolability of some compounds, analyses were performed with a temperature ramp-up (50°C every 15 sec) over 2 min. The temperature range covered was therefore 100–400°C with 120 scans in the range *m/z* 100–2,000. Source parameters were optimized as follows: a nebulization gas (nitrogen) pressure of 2.5 bars and a dry gas flow rate at 2.5 $L.min^{-1}$. Voltages were set to: 500 V for the transfer capillary, −500 V for the end plate offset, with a 2,000 V charging voltage and a 4,000 V working voltage. An ion cooler of 175 $V_{p\text{-}p}$ was applied on the pusher. The corona discharge was set to 500 nA for positive ionization and 2,000 nA for negative ionization. External calibration of the spectrometer was done with PEG600 in positive mode and PEG diacid 600 in negative mode. Lock-mass calibration was applied on palmitic acid by post-processing with R-script.[27] During the batch two replicates were performed to obtain a total of eight acquisitions on the merged data for interpretation. Experiments were performed as a single batch with a thermal desorption to noise level between each run. No loss of sensitivity was observed on controls.

2.5 | Bioinformatic data processing

Thermo Scientific *.RAW files were converted to *.mzXML using readw 4.3.1 and Bruker *.d folders were converted to *.mzXML using Bruker CompassXport 3.0.6.9 from the command line. The obtained files were processed with R-script and Microsoft Visual Basic, and following the Seven Golden Rules of MF determination,[16] every step was controlled manually while encoding the scripts, and exported in the form of *.csv files.

Peak lists were extracted from the *.mzXML files using R packages `xcms`,[28-30] `MSnbase`,[31] and `CAMERA`,[32] and automated instrument detection was performed with the `readMzXmlData`[33] package. The peak picking parameters were optimized for each instrument. Isotopic contributions calculation and clustering followed by deisotoping were performed with a 3 ppm tolerance using element restrictions depending on *m/z* as described in the Seven Golden Rules. For this purpose the mass ranges were refined according to the compounds referenced in the online Dictionary of Natural Products (DNP) v26.2[34] (Table 1). After an in-depth study of the mass spectra, it appeared that isotopic contributions could not be seen for monoisotopic ions of less than 0.01% relative intensity, so this value was set as a threshold for the calculation of isotopic clusters.

The MFs were then calculated by querying the online platform ChemCalc[35] with R-script, taking into account the calculated isotopic patterns, allowing an error of four carbons and two nitrogens.

Mass range [Da]	C max	H max	N max	O max	S max	Cl max
<200	15	30	8	7	6	4
<400	30	58	10	14	12	7
<600	42	86	13	21	12	8
<800	56	108	16	25	20	10
<1,000	66	126	25	37	20	11
<1,500	100	182	26	44	20	11

TABLE 1 Element restriction ranges established from the online dictionary of natural products v26.2

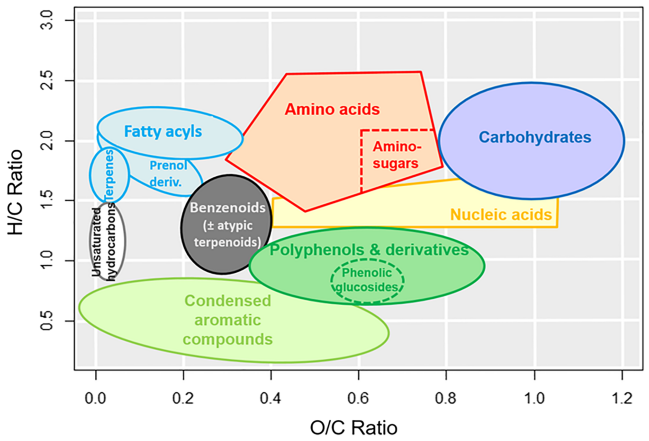

FIGURE 1 Identification of the chemical groups on the Van Krevelen diagram.

$[M + Na]^+$ adducts were further accounted for when generating the formulae for ESI-MS. When no isotope pattern was detected, Table 1 features were considered. However, sulfur and chlorine were not considered unless detected. The absolute mass range error was set to 1.0 milli-unified atomic mass (mu) for orbitrap data (DI-ESI-MS) and 1.7 mu for Q-TOF data (ASAP-MS). Based on the double bond equivalent (DBE) the script filtered out the formulae corresponding to radical ions for ESI-MS. The results were coherent with manual MF determination of known compounds and yielded most often a single formula, though the script was able to calculate the five best formulae.

The different elemental ratios were then calculated with Visual Basic in order to filter the formulae according to the Seven Golden Rules to remove the potentially incoherent ones. An adduct correction was applied according to the formulae and DBE with the following considered adducts: ASAP-MS: $M^{+\bullet}$, $[M + H]^+$, $M^{-\bullet}$, and $[M\text{-}H]^-$; ESI-MS: $[M + H]^+$, $[M + Na]^+$, $[M\text{-}H]^-$, and $[M + Cl]^-$. The corresponding exact molecular masses were subsequently calculated.

Chemical classes associated with the VK diagram were retrieved from the literature and double-checked against an in-house database of lichen compounds. The complete project is available[12] (see **Technical validation** section). The *VK coordinates*, i.e., the *H/C and O/C ratios*, were then imported in R-script and merged in a single matrix that can be filtered by all experimental variables. A rectangle approximation of the chemical groups presented in Figure 1 was applied to tag the detected compounds, which were filtered for plotting in the form of a histogram (relative proportion within a method) stacked with a heatmap (absolute count of detected features). The plots were created with R package `plot3D`[36] and were made interactive with `plot3Drgl`.[37] Although the presented plots were constructed with the merged data of all lichens, the provided scripts allow for species filtering (e.g., Figure S2). The VK coordinates were also used to plot the VK diagrams using R-script.

The entire processed dataset is available at https://osf.io/6pyuq/ (dataset_solvents_comp_publi1.tsv) along with sample files for Q-Orbitrap and Q-TOF data in the *.mzXML format. The scripts are deposited at https://github.com/siollivier/directacquisitionproject.

2.6 | Technical validation

2.6.1 | Database establishment

An in-house database of lichen compounds was compiled from the literature. The total number of structures contained in this compiled database is about 2,000 entries.[12] The database will be provided by the authors upon reasonable request.

The structural information was translated into InChIKey, a particularly popular format in chemoinformatics, because it is standardized and of fixed length, allowing easy data processing (example: mycosporine serinol, VVTDHOIRNPCGTH-NSHDSACASA-N).

A detailed classification of the lichen compounds was then obtained by submitting these InChIKeys to ClassyFire,[14] a tool to obtain a hierarchical classification of compounds, through the `classyfireR` package.[38] This structure-based bioinformatics approach allows for a comprehensive result through the establishment of a chemical taxonomy – in hierarchical order: chemical kingdom, superclass, class, subclass, and additional levels 5–9.

2.6.2 | Evaluation of the method against a state-of-the-art classification tool

The accuracy of the classification established in Figure 1 was examined in comparison to this database of lichen compounds. Within the database, compounds were selected according to different levels of their ClassyFire classification, which was compared to the classification obtained with VK.

The same level of precision cannot be expected from a classification based only on the MF. However, depending on the structure of the compounds, it is possible to expect a result in one or more classes (more or less specific) of this diagram. Thus, some areas of the diagram (i.e., benzenoids or prenyl derivatives) can be considered as areas that extend more specific ones. During the evaluation of the protocol, the compounds were considered as correctly classified if their VK annotation was in accordance with the expected matches between ClassyFire and VK that are shown in Table 2.

TABLE 2 Matches between ClassyFire and the Van Krevelen diagram for the most common lichen metabolites. The matches were determined to fit properly with the usual classification of lichen compounds by Huneck and Yoshimura[21]

ClassyFire classification (level)	Expected area(s) in the Van Krevelen diagram
Amino acids and analogs (subclass)	Amino acids; nucleic acids
Anthraquinones (subclass)	Condensed aromatic compounds
Benzene derivatives (class)	***Polyphenols and derivatives***; benzenoids
Carbohydrates and conjugates (subclass)	Carbohydrates
Chromones (level 5)	***Polyphenols and derivatives***; benzenoids
Depsides and depsidones (class)	***Polyphenols and derivatives***; benzenoids
Dibenzofurans (subclass)	Condensed aromatic compounds; benzenoids
Fatty acyls (class)	Fatty acyls; prenol derivatives
Prenol lipids (class)	Terpenes; prenol derivatives; unsaturated hydrocarbons
Xanthones (level 7)	Condensed aromatic compounds

3 | RESULTS AND DISCUSSION

3.1 | Determination and validation of the Van Krevelen chemical groups

First, a search was conducted in the literature to identify the positioning of the defined chemical groups on the VK diagram.[18,19,39–41] These bibliographic results were then refined according to a database organized with ClassyFire, and the final ranges are specified in Figure 1. The database used to validate these annotations mostly contains compounds of MW < 500 Da, including mainly, in terms of ClassyFire classes, depsides and depsidones (>20%), as illustrated in Figure 2.

In order to guarantee the quality of the following results, it is first necessary to evaluate the accuracy of the classification on datasets not acquired in DDA. The proportion of correctly classified molecules in each class is an effective way to perform this validation.

However, two biases to this estimation should be considered. (1) The classification being based on H/C and O/C ratios, classes containing a large number of heteroatoms (N, S, etc.) such as amino acids are more likely to be incorrectly classified. Others have addressed this issue by including various elemental ratios, but this promising approach has yet to achieve the same level of specificity for classification.[42] (2) Some ClassyFire classifications include very structurally diverse derivatives within the same class, particularly for compounds with a lipid or carbohydrate function.

The proportions of molecules correctly classified in each of the classes considered are presented in Figure 3. As expected, amino acids and analogs, fatty acyls, and carbohydrates have a lesser overlap between the two classifications, with respectively 56%, 59%, and 68% of compounds being correctly classified.

On the other hand, all the other structural classes considered have an overlap of more than 70%. For four of the 10 structural types considered, the similarity between the two classifications is even higher than 90%. These are benzenoid derivatives, chromones,

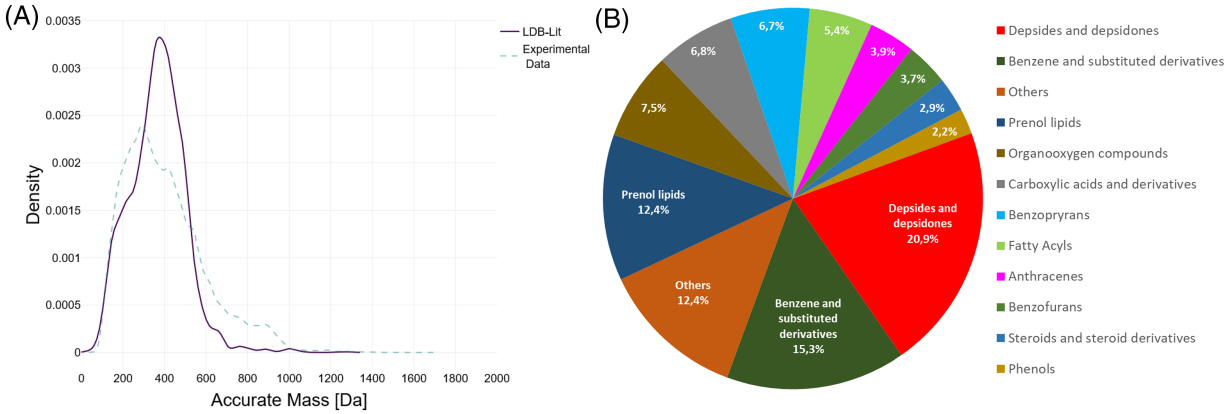

FIGURE 2 (A) The distribution of the molecular weights of the compounds contained in the validation database (LDB-lit, solid line) shows a good overlap with the experimental data (dotted line). (B) The ClassyFire classes of the compounds in the LDB-lit illustrate the diversity of the molecules used for technical validation.

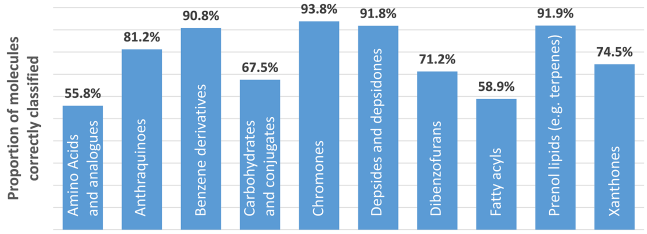

FIGURE 3 Proportions of molecules in the database accurately classified by the Van Krevelen diagram (in accordance with Table 2).

depsides, and depsidones, as well as prenol lipids, which include terpenes. These chemical families are among the most frequently reported in lichens, as illustrated in the recently published tandem mass spectra database of the most common lichen compounds.[12]

The encouraging results of the method provided by processing non-experimental data gave us the incentive to proceed to a practical evaluation. In the following case study, this method is used to obtain a rapid evaluation of the diversity of compounds detected by multiple ionization techniques, presenting a comparison of results from two DI-ESI-MS conditions vs. ASAP-MS.

3.2 | Case study: Evaluation of the metabolic diversity of lichen extracts

In order to cover a large panel of structures from lichen extracts, four lichen samples known to have very distinct metabolite profiles were chosen (the numbers of compounds in the ClassyFire classes are given in Table S2 for each lichen). Protocols used for each lichen species (two single-step and two three-step ones) were established to have a comparison with a simple extraction generally used in chemotaxonomic studies in lichenology and more exhaustive extractions (pooling successive extracts from polar to apolar ones) (Figure S1). These extracts were analyzed with DI-ESI-MS and ASAP-MS to compare the performance of these techniques to reveal lichen compounds and evaluate their distribution in structural families (Figure S2).

The DI-ESI-MS experiments were conducted with two ionization solvents, acetone and methanol, since this aspect of the experiment heavily impacts the compound detection. Indeed, with positive ion mode data, principal component analysis (PCA) shows that the two ionization solvents form distinct groups on PC2 (Figure S3). PC1 clearly differentiates DI-ESI-MS from ASAP-MS analysis and post-treated data with an adduct correction resulted in a slightly better clustering of samples with regard to raw data. While the positive ion mode detects a huge number of compounds when compared to the negative ion mode, the VK diagram provides a broad and clear overview of the chemical diversity of the diverse chemical families in lichens. The complementarity of these three methods is also revealed through the distinct zones mostly covered by these three MS conditions on the VK diagram with all discriminant coordinates (Figure S4).

In other words, a single detection mode is not sufficient to cover the metabolic diversity of lichen compounds and each technique is more or less suitable for a class of compounds to be revealed. This assumption was verified using a bioinformatic quantification of the number of molecules ionized in various samples obtained with different extraction protocols: depending on their MF, a structural class was assigned to the compounds according to the cartography presented Figure 1.

With regard to the relative performance of the extraction protocols compared in this study the quantitative and the qualitative aspects are considered. Comparing extractions with a single solvent, yields are higher when a polar protic solvent (i.e., methanol) is used instead of a polar aprotic solvent (i.e., acetone). The CAM and CAW extractions gave yields in the same range compared to a single methanol extraction (Figure S1).

Considering the performance of the MS techniques used to reveal the composition of extracts, the results obtained with the two multi-step solvents were analyzed, which are considered to be the more exhaustive. In Figure 4 ASAP-MS allowed the detection of more compounds than ESI-MS in negative mode (average number of ions: 424/run for ASAP-MS vs. 116/run for ESI-MS in acetone), but fewer in positive mode (average: 482/run for ASAP-MS vs. 1,434/run for ESI-MS in acetone). Furthermore, these results are coherent with what could be expected when considering the protic solvent selected, and the most appropriate extraction and ionization methods for each class of compounds are summarized in Table 3. In addition, the comparison with the in-house database[12] exhibits differences for fatty acyls or amino acids, as examples, with higher frequencies in the experimental data than in the database.

3.2.1 | Regarding the extraction protocols

The successive extraction steps method appears to be better suited than the methanol extraction to gather terpenes and prenol derivatives (2.0 and 1.5 times more in positive ASAP-MS, respectively), while 1.3 times more carbohydrates were extracted with water (negative ESI-MS in methanol).

A comparison with the single-step extractions (Figure S5) shows that an acetone extraction would appear as a good choice for studies targeting polyphenols and derivatives or condensed aromatic structures as well as terpenes. On the other hand, as methanol has the closest extraction profile to that of the successive solvent extraction and comparable yields, it seems to be a good compromise. However as expected with a protic solvent fewer terpenes are extracted with methanol.

3.2.2 | Regarding the MS methods

Compared to ESI-MS, ASAP-MS favors the ionization of terpenes (relative frequency [r.f.] within an ionization method up to 20%) and unsaturated hydrocarbons (r.f. 10%) in positive mode and benzenoids (r.f. 35%) in negative mode. However, ASAP-MS appears less

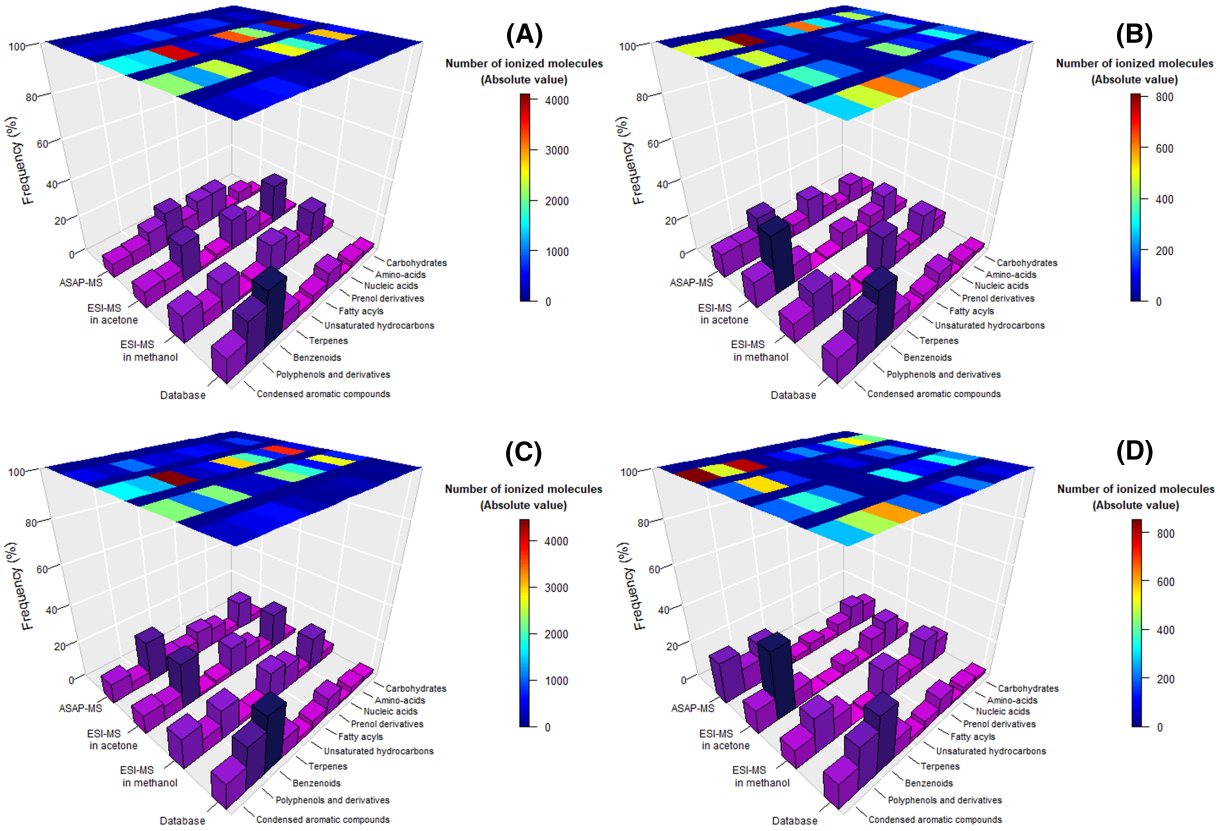

FIGURE 4 Evaluation of the chemical diversity for the merged data of the three-step extractions: "cyclohexane–acetone–methanol" in positive mode (A) and negative mode (B), and "cyclohexane–acetone–water" in positive mode (C) and negative mode (D). Both the relative frequency for each technique (histogram, vertical axis) and the absolute number of detected ions (heatmap) are presented. The relative frequency represents the proportion of a chemical class within a given ionization method. The database content is proposed in comparison to show the existing potential in new identifications.

TABLE 3 An overview of the most efficient parameters in this study for the extraction and MS analysis of lichen metabolites, with regards to the number of compounds ionized and the amount of other metabolites that may hinder the interpretation for each structural class

Class	Extraction	Ionization	MS polarity
Carbohydrates	CAW	ESI in methanol	NEG
Amino acids	Methanol	ESI in acetone	POS
Nucleic acids	CAW	ESI in acetone	NEG
Prenol derivatives	CAM	ASAP (APCI)	POS
Fatty acyls	Methanol	ESI in methanol	NEG
Unsaturated Hydrocarbons	CAM	ASAP (APCI)	POS
Terpenes	CAM or acetone	ASAP (APCI)	POS
Benzenoids	Acetone	ESI in acetone	POS
Polyphenols and derivatives	Acetone	ESI in acetone	NEG
Condensed aromatic compounds	Acetone	ESI in methanol	POS

favorable for polyphenols and derivatives but, interestingly, quite favorable for condensed aromatic compounds (up to r.f. 20% in some conditions; see Figure 4d).

This piece of data also shows differences between the two DI-ESI-MS ionization solvents that may be of use for targeted studies: in negative mode, carbohydrate and fatty acyl ionization is superior in methanol (15% vs. 10% and 20% vs. 10% r.f., respectively), whereas that of polyphenols and derivatives and condensed aromatic compounds is better in acetone (40% vs. 25% and 15% vs. 10%, respectively). Differences are less marked in positive ionization, except for the condensed aromatic structures that are better ionized in methanol (>15% vs. 10%). Such compounds are common occurrences in lichens (e.g., depsides for polyphenols and derivatives and xanthones for condensed aromatic compounds).[21,43]

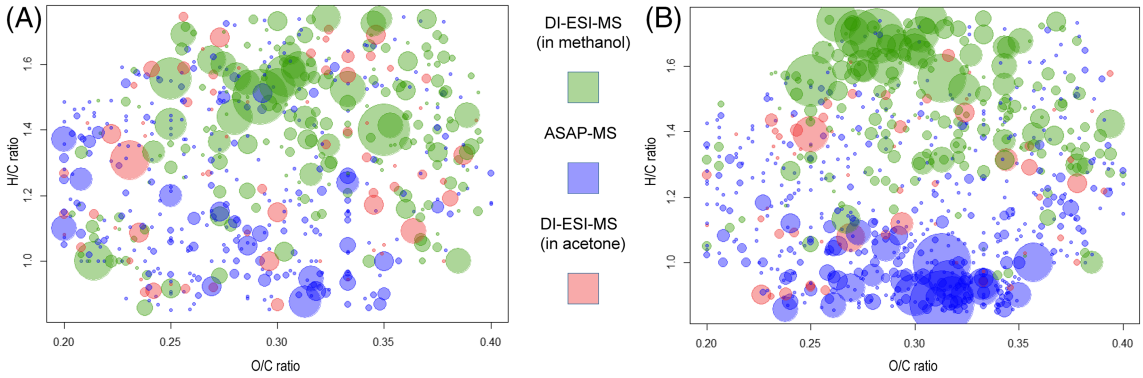

FIGURE 5 Extracted Van Krevelen diagram for benzenoids, i.e., in the (O/C 0.2–0.4; H/C 0.8–1.8) range, in all three ionization methods for the acetone (A) and cyclohexane–acetone–methanol extracts (B). The size of the circle, represented by a coefficient of expansion (cex), is proportional to the number of occurrences of the (O/C, H/C) coordinates without correction factor (100 gives a cex of 100). The colors (green, blue, and red, alpha of 0.4) indicate respectively discriminant VK coordinates for DI-ESI-MS in methanol, ASAP-MS, and DI-ESI-MS in acetone ionization mode.

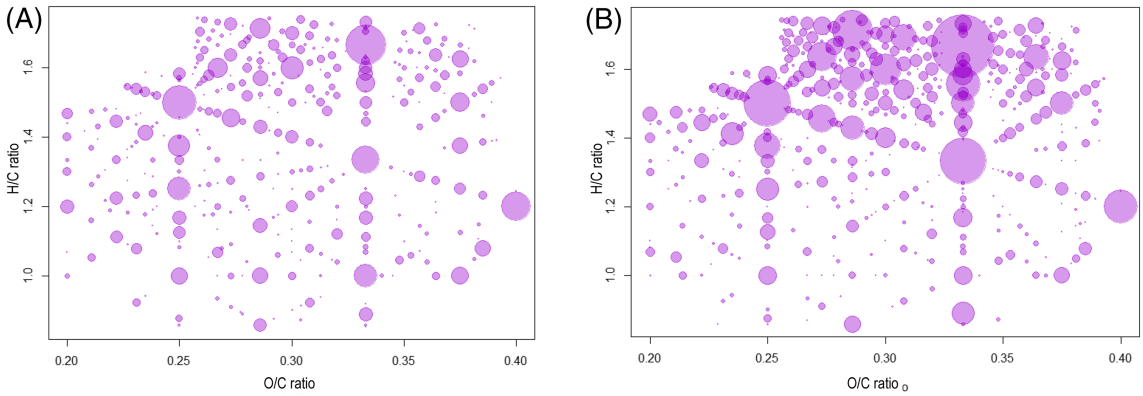

FIGURE 6 Extracted Van Krevelen diagram for benzenoids, i.e., in the (O/C 0.2–0.4; H/C 0.8–1.8) range, in all three ionization methods for the acetone (A) and cyclohexane–acetone–methanol extracts (B). The size of the circle is proportional to the number of occurrences of the (O/C, H/C) coordinates with a correction factor of 0.1 (100 gives a cex of 10). Non-discriminant VK coordinates for a single ionization mode are plotted in violet.

Furthermore, in positive mode there appears to be a similar ionization profile for benzenoids in all ionization methods (Figure 4, Figure S5), questioning the complementarity of the methods in this aspect. A referral to the VK diagram however reveals that the ionized compounds have some discriminant elemental ratios with each method (Figure 5). VK discriminant coordinates are clearly found in low H/C ratio for ASAP-MS and in high H/C ratio for DI-ESI-MS in methanol, whereas DI-ESI-MS in acetone as few discriminant coordinates, showing a complementarity within the ionization modes. A referral to the VK diagram however reveals that some elemental ratios are common to two or three ionization modes (Figure 6). Moreover, an overall higher number of occurrences in acetone extract is clearly observed, with a specificity in high H/C ratio – once again showing the usefulness of the VK diagram for NP metabolomics. To illustrate the potential of the use of ambient MS for validation or new identification of NPs, in comparison with the in-house database, classical expected compounds but also new coordinates are found in DI-ESI-MS and ASAP-MS as proofs of principle (Figures S6–S10).

Overall, the interest of the VK diagram was demonstrated for the structural classification of metabolites (without the need to acquire tandem mass spectra data), and its applicability was shown with real-life cases by studying the chemical composition of lichens.

ACKNOWLEDGEMENTS

The authors thank Isabelle Rouaud (ISCR, CorInt, Rennes) for her technical assistance regarding the extraction protocols.

AUTHOR NOTES

SO, PJ, FLD, JB, and NLY designed the experiments. SO and FLD selected the lichen material, which was identified by JB. DO optimized the ASE protocol. SO, PJ, and FL carried out the experiments. SO and NLY encoded the R-scripts and Visual Basic macro used for data processing. DO compiled the database for validation. DO and SO curated the database. All authors contributed to the redaction of the manuscript. None of the authors declare any competing financial interest.

DATA AVAILABILITY STATEMENT

The data that support the findings of this study are available in the supporting information of this article. Further data are available from the corresponding author upon reasonable request.

ORCID

Simon Ollivier https://orcid.org/0000-0002-7671-1736
Damien Olivier-Jimenez https://orcid.org/0000-0002-6363-0857
Joël Boustie https://orcid.org/0000-0002-3936-3859
Françoise Lohézic-Le Dévéhat https://orcid.org/0000-0003-4307-4942
Nicolas Le Yondre https://orcid.org/0000-0002-0783-3668

REFERENCES

1. Wolfender J-L, Marti G, Thomas A, Bertrand S. Current approaches and challenges for the metabolite profiling of complex natural extracts. *J Chromatogr A*. 2015;1382:136-164. doi:10.1016/j.chroma.2014.10.091
2. Wolfender JL, Nuzillard JM, Van der JH, Renault JH, Bertrand S. Accelerating metabolite identification in natural product research: toward an ideal combination of LC-HRMS/MS and NMR profiling, in silico databases and chemometrics. *Anal Chem*. Published online November 2018. 91(1):704-742. doi:10.1021/acs.analchem.8b05112
3. Sarker SD, Latif Z, Gray AI. Natural Product Isolation. In: Sarker SD, Latif Z, Gray AI, eds. *Natural Products Isolation*. Methods in Biotechnology. Humana Press; 2005:1-25. doi:10.1385/1-59259-955-9:1
4. Choi YH, Verpoorte R. Metabolomics: What You See is What you Extract. *Phytochem Anal*. 2014;25(4):289-290. doi:10.1002/pca.2513
5. Basmadjian C, Zhao Q, Bentouhami E, et al. Cancer wars: natural products strike back. *Front Chem*. 2014;2:20. doi:10.3389/fchem.2014.00020
6. Ernst M, Kang KB, Caraballo-Rodríguez AM, et al. MolNetEnhancer: Enhanced Molecular Networks by Integrating Metabolome Mining and Annotation Tools. *Metabolites*. 2019;9(7):144. doi:10.3390/metabo9070144
7. Allard P-M, Genta-Jouve G, Wolfender J-L. Deep metabolome annotation in natural products research: towards a virtuous cycle in metabolite identification. *Curr Opin Chem Biol*. 2017;36:40-49. doi:10.1016/j.cbpa.2016.12.022
8. Wang M, Carver JJ, Phelan VV, et al. Sharing and community curation of mass spectrometry data with Global Natural Products Social Molecular Networking. *Nat Biotechnol*. 2016;34:828-837. doi:10.1038/nbt.3597
9. Wandy J, Zhu Y, van der Hooft JJJ, Daly R, Barrett MP, Rogers S. Ms2lda.org: web-based topic modelling for substructure discovery in mass spectrometry. *Bioinformatics*. 2018;34(2):317-318. doi:10.1093/bioinformatics/btx582
10. van der HJJJ, Wandy J, Barrett MP, Burgess KEV, Rogers S. Topic modeling for untargeted substructure exploration in metabolomics. *Proc Natl Acad Sci*. 2016;113(48):13738-13743. doi:10.1073/pnas.1608041113
11. Ramos AEF, Le Pogam P, Alcover CF, et al. Collected mass spectrometry data on monoterpene indole alkaloids from natural product chemistry research. *Sci Data*. 2019;6(1):1-6. doi:10.1038/s41597-019-0028-3
12. Olivier-Jimenez D, Chollet-Krugler M, Rondeau D, et al. A database of high-resolution MS/MS spectra for lichen metabolites. *Sci Data*. 2019;6(1):1-11. doi:10.1038/s41597-019-0305-1
13. Allard P-M, Péresse T, Bisson J, et al. Integration of Molecular Networking and In-Silico MS/MS Fragmentation for Natural Products Dereplication. *Anal Chem*. 2016;88(6):3317-3323. doi:10.1021/acs.analchem.5b04804
14. Djoumbou Feunang Y, Eisner R, Knox C, et al. ClassyFire: automated chemical classification with a comprehensive, computable taxonomy. *J Chem*. 2016;8(1):61. doi:10.1186/s13321-016-0174-y
15. Bilbao A, Varesio E, Luban J, et al. Processing strategies and software solutions for data-independent acquisition in mass spectrometry. *Proteomics*. 2015;15(5–6):964-980. doi:10.1002/pmic.201400323
16. Kind T, Fiehn O. Seven Golden Rules for heuristic filtering of molecular formulas obtained by accurate mass spectrometry. *BMC Bioinf*. 2007;8(1):105. doi:10.1186/1471-2105-8-105
17. Van Krevelen DW. Graphical-statistical method for the study of structure and reaction processes of coal. *Fuel*. 1950;29:269-284.
18. Roullier-Gall C, Witting M, Gougeon RD, Schmitt-Kopplin P. High precision mass measurements for wine metabolomics. *Front Chem*. 2014:2. doi:10.3389/fchem.2014.00102
19. Roullier-Gall C, Lucio M, Noret L, Schmitt-Kopplin P, Gougeon R. How Subtle Is the "Terroir" Effect? Chemistry-Related Signatures of Two "Climats de Bourgogne". *PLoS ONE*. 2014;9(5):e97615. doi:10.1371/journal.pone.0097615
20. Brockman SA, Roden EV, Hegeman AD. Van Krevelen diagram visualization of high resolution-mass spectrometry metabolomics data with OpenVanKrevelen. *Metabolomics*. 2018;14(4):48. doi:10.1007/s11306-018-1343-y
21. Huneck S, Yoshimura I. *Identification of Lichen Substances*. Berlin Heidelberg: Springer; 1996 Accessed February 17, 2019. http://public.eblib.com/choice/publicfullrecord.aspx?p=3097560
22. Kitson E, Kew W, Ding W, Bell NGA. PyKrev: A Python Library for the Analysis of Complex Mixture FT-MS Data. *J Am Soc Mass Spectrom*. 2021;32(5):1263-1267. doi:10.1021/jasms.1c00064
23. Honegger R. The Lichen Symbiosis—What is so Spectacular about it?*. *Lichenologist* 1998;30(3):193-212. doi:10.1006/lich.1998.0140
24. Boustie J, Grube M. Lichens—a promising source of bioactive secondary metabolites. *Plant Genet Resour*. 2005;3(2):273-287. doi:10.1079/PGR200572
25. Ranković B, Kosanić M. Lichens as a Potential Source of Bioactive Secondary Metabolites. In: Ranković B, ed. *Lichen Secondary Metabolites: Bioactive Properties and Pharmaceutical Potential*. Springer International Publishing; 2015:1-26. doi:10.1007/978-3-319-13374-4_1.
26. Lutzoni F, Pagel M, Reeb V. Major fungal lineages are derived from lichen symbiotic ancestors. *Nature*. 2001;411(6840):937-940. doi:10.1038/35082053
27. R Core Team. *R: A Language and Environment for Statistical Computing*. Vienna, Austria: R Foundation for Statistical Computing; 2018. https://www.R-project.org/
28. Smith CA, Want EJ, OMaille G, Abagyan R, Siuzdak G. XCMS: processing mass spectrometry data for metabolite profiling using nonlinear peak alignment, matching, and identification. *Anal Chem*. 2006;78(3):779-787. doi:10.1021/ac051437y
29. Tautenhahn R, Böttcher C, Neumann S. Highly sensitive feature detection for high resolution LC/MS. *BMC Bioinf*. 2008;9(1):504. doi:10.1186/1471-2105-9-504
30. Benton HP, Want EJ, Ebbels TMD. Correction of mass calibration gaps in liquid chromatography–mass spectrometry metabolomics data. *Bioinformatics*. 2010;26(19):2488-2489. doi:10.1093/bioinformatics/btq441
31. Gatto L, Lilley KS. MSnbase-an R/Bioconductor package for isobaric tagged mass spectrometry data visualization, processing and quantitation. *Bioinformatics*. 2012;28(2):288-289. doi:10.1093/bioinformatics/btr645
32. Kuhl C, Tautenhahn R, Böttcher C, Larson TR, Neumann S. CAMERA: an integrated strategy for compound spectra extraction and annotation of liquid chromatography/mass spectrometry data sets. *Anal Chem*. 2012;84(1):283-289. doi:10.1021/ac202450g

33. Gibb S. ReadMzXmlData: *Reads Mass Spectrometry Data in MzXML Format*. 2015. Accessed February 21, 2019. https://CRAN.R-project.org/package=readMzXmlData
34. Dictionary of Natural Products 26.2. Published April 13, 2018. Accessed April 13, 2018. https://dnp.chemnetbase.com/faces/chemical/ChemicalSearch.xhtml
35. Patiny L, Borel A. ChemCalc: A Building Block for Tomorrows Chemical Infrastructure. *J Chem Inf Model*. 2013;53(5):1223-1228. doi:10.1021/ci300563h
36. Soetaert K. Plot3D: Plotting Multi-Dimensional Data; 2017. Accessed February 21, 2019. https://CRAN.R-project.org/package=plot3D
37. Soetaert K. *Plot3Drgl: Plotting Multi-Dimensional Data - Using "Rgl."*; 2016. Accessed February 21, 2019. https://CRAN.R-project.org/package=plot3Drgl
38. Wilson T, Finch J. *ClassyfireR: R Interface to the ClassyFire RESTful API*.; 2019. Accessed August 16, 2019. https://CRAN.R-project.org/package=classyfireR
39. D'Andrilli J, Cooper W, Foreman C, Marshall AG. An ultrahigh-resolution mass spectrometry index to estimate natural organic matter lability. *Rapid Commun Mass Spectrom*. 2015;29:2385-2401. doi:10.1002/rcm.7400
40. Kuhnert N, Dairpoosh F, Yassin G, Golon A, Jaiswal R. What Is under the Hump? Mass Spectrometry Based Analysis of Complex Mixtures in Processed Food – Lessons from the Characterisation of Black Tea Thearubigins. *Coffee Melanoid Caramel*. 2013;4(8):1130-1147. doi:10.1039/c3fo30385c
41. Lu Y, Li X, Mesfioui R, et al. Use of ESI-FTICR-MS to Characterize Dissolved Organic Matter in Headwater Streams Draining Forest-Dominated and Pasture-Dominated Watersheds. *PLoS ONE*. 2015;10(12):e0145639. doi:10.1371/journal.pone.0145639
42. Rivas-Ubach A, Liu Y, Bianchi TS, Tolić N, Jansson C, Paša-Tolić L. Moving beyond the van Krevelen Diagram: A New Stoichiometric Approach for Compound Classification in Organisms. *Anal Chem*. 2018;90(10):6152-6160. doi:10.1021/acs.analchem.8b00529
43. Le Pogam P, Boustie J. Xanthones of Lichen Source: A 2016 Update. *Molecules*. 2016;21(3):294. doi:10.3390/molecules21030294

SUPPORTING INFORMATION

Additional supporting information can be found online in the Supporting Information section at the end of this article.

How to cite this article: Ollivier S, Jéhan P, Olivier-Jimenez D, et al. New insights into the Van Krevelen diagram: Automated molecular formula determination from HRMS for a large chemical profiling of lichen extracts. *Phytochemical Analysis*. 2022;33(7):1111-1120. doi:10.1002/pca.3163